

SOME THEORETICAL ASPECTS OF RF SUPERCONDUCTIVITY*

J. P. Turneaure

W. W. Hansen Laboratories of Physics, High Energy Physics Laboratory, Stanford University, Stanford, California 94305 USA

Abstract

The work toward the development of superconducting accelerators and particle separators has led to a considerable improvement in our understanding of rf superconductivity. This paper will discuss our present understanding of rf superconductivity with emphasis on those topics that relate to accelerating devices.

1. Introduction

Superconducting rf cavities have been suggested for use in building a wide range of accelerating devices: examples are electron microscopes of a few MeV and linear proton accelerators in combination with recirculation to produce several thousand GeV protons¹). Many other accelerating devices using superconducting rf cavities at energies in the range of 1 MeV to 1000 GeV are under consideration. A number of these are now in various stages of construction and development^{2),3),4)}. The work toward the development of these accelerators and particle separators has led to a considerable improvement in our understanding of rf superconductivity. This paper will discuss our present understanding of rf superconductivity with emphasis on those topics that relate to accelerating devices. Technological details of a superconducting materials nature will be avoided in the discussion.

2. Relation of Experiment to Theory

There are a number of experimental parameters at ones disposal which can either be controlled (at least to some degree) or which can be measured. In an experiment, one typically determines the cavity shape and mode, the metallurgical condition of the superconductor, and the microwave frequency and field in the cavity. There are in addition other parameters that may be controlled in an experiment. Examples are the ambient field on the cavity at cool down through the superconducting transition temperature T_c , the quality of the vacuum in the cavity, the density of He gas admitted into the cavity, etc. After setting the above experimental parameters, one can in turn measure the unloaded Q , Q_0 , and resonant frequency ω_0 of the cavity. One can in addition measure other factors in a cavity experiment such as x-radiation (including intensity, energy spectrum, and spatial distribution), distribution of heat dissipation, phonons, electron currents within the cavity volume, etc.

Unfortunately there is no unique way to relate experimental measurements to specific properties of a superconductor. For instance, the experimental Q_0 is the result of the total power dissipation in a cavity. By a Q_0 measurement

alone, one can not determine what fraction of the power dissipation goes into a specific dissipation mechanism. One must always make assumptions (which may perhaps be verified by additional experiments) as to the types of power dissipation actually occurring.

One of the most important types of power dissipation is that coming from the presence of rf currents near the surface of the superconductor. This type of power dissipation can be characterized by a complex surface impedance Z .

$$Z = R + i X \quad , \quad (1)$$

where $i = \sqrt{-1}$. The real part of Z is called the surface resistance R ; and the imaginary part of Z is called the surface reactance X . The surface resistance is related to the power dissipation P_{dis} in a cavity by

$$P_{dis} = \frac{1}{2} R \int_{\text{surface}} \left(\frac{c}{4\pi} H \right)^2 da \quad , \quad (2)$$

where the units are cgs-Gaussian, and the integral is over the surface of the cavity. In Eq. (2), the quantity under the integral sign is the square of the surface current (in cgs-Gaussian units the surface current is $[c/4\pi]H$). The surface reactance can be related to a reactive skin depth; however it is not of much interest in the discussion of accelerating devices and it will not be discussed further.

The surface resistance can be related to the Q_0 of a cavity assuming there is only rf surface current dissipation and that the surface resistance is uniform over the cavity surface. (These assumptions are often not correct.) With these assumptions

$$R = \Gamma / Q_0 \quad , \quad (3)$$

where Γ is a geometrical factor depending on cavity shape and mode. Γ can be expressed by integrals over the magnetic field H for the particular mode of interest:

$$\Gamma = \frac{4\pi}{c^2} \int_{\text{volume}} H^2 dv / \int_{\text{surface}} H^2 da \quad , \quad (4)$$

where Eq. (4) is in cgs-Gaussian units.

Pb and Nb superconductors are of most interest for accelerating devices because of their potential high rf magnetic fields. Various methods have developed for manufacturing these superconducting cavities^{5),6),7),8),9),10)}; however, no details will be given here.

3. The Low Field BCS Surface Resistance

The properties of superconductors at low magnetic fields are approximated to a good degree by the BCS theory of superconductivity¹¹). The superconducting surface impedance is no exception. There are some results from the BCS theory that give a rather clear idea of how the temperature dependence of the superconducting surface resistance arises. Figure 1 shows the density of electron states in a small region near the Fermi surface. The BCS density of states has some very important properties: there are no electron states available for energies between ϵ_1 and ϵ_2 , the Fermi energy ϵ_f lies half way between ϵ_1 and ϵ_2 (an energy Δ from each), and there are inverse square root singularities in the density of states at the energy gap edges, ϵ_1 and ϵ_2 . As shown in Fig. 1 for $T = 0^\circ\text{K}$, the electrons in the superconductor occupy all the states below the lower gap edge ϵ_1 and none of the states above the upper gap edge ϵ_2 . Since electrons obey Fermi-Dirac statistics, only one electron of each spin may occupy each space state. At 0°K , this means that an electron must acquire an energy of 2Δ in order to make a transition to a new state. Since at low field only single photon absorption is probable, a photon of minimum frequency $2\Delta/h$ (h is Planck's constant) is necessary to excite an electron to a new state. This frequency is about 7×10^{11} Hz for Pb and Nb. Since superconducting accelerator devices generally involve frequencies of less than 10^{10} Hz; at 0°K there will be no direct transitions of electrons across the energy gap 2Δ , and hence the BCS surface resistance at 0°K will be zero.

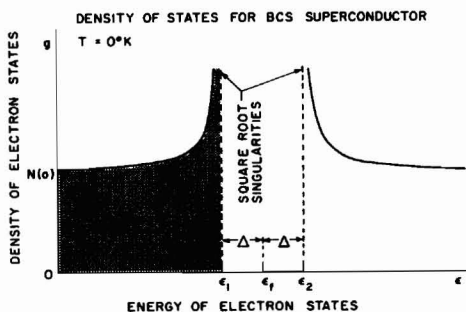


Fig. 1. Density of electron states for a BCS superconductor with the occupied states at $T = 0^\circ\text{K}$ indicated.

At finite temperature, electrons will be thermally excited across the energy gap. Also the energy gap will decrease with increasing temperature until it reaches zero at the superconducting transition temperature T_c . The number of electrons excited across the energy gap is proportional to the Fermi-Dirac distribution function, which can be ap-

proximately written for low temperatures ($T < 0.5 T_c$) as $\exp(-\Delta/k_B T)$, where k_B is the Boltzmann constant. Figure 2 indicates the occupied states at a finite temperature. It is clear from Fig. 2 that electrons can be excited to unfilled states very close in energy to their original energy. Thus at finite temperatures, photons of low frequency ($< 10^{10}$ Hz) can excite electrons to higher states, and power dissipation occurs when these electrons thermally relax to lower energy states again. For low temperatures ($T < 0.5 T_c$), the superconducting surface resistance R_{BCS} is very closely proportional to the number of electrons thermally excited across the energy gap: $R_{BCS} \propto \exp(-\Delta/k_B T)$.

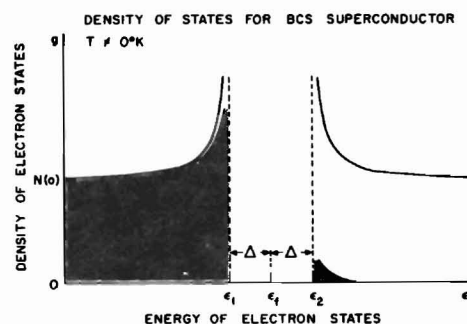


Fig. 2. Density of electron states for a BCS superconductor with the occupied states for $T \neq 0^\circ\text{K}$ indicated.

Another important result of the theory of superconductivity is shown in Fig. 3. When a magnetic field (dc or rf) is applied to the surface of a superconductor, the magnetic field does not penetrate the bulk of the superconductor except near the surface where shielding currents arise. The current density and magnetic field decrease approximately exponentially as a function of distance from the surface according to the form $\exp(-x/\lambda)$. The distance λ is called the penetration depth. At dc the electric field in the superconductor is zero; however, for rf applied magnetic fields, the electric field in the superconductor is non-zero but small due to magnetic induction. The electric field is proportional to λ and ω , and also decreases approximately exponentially. It is this electric field that couples photons to the electrons.

Expressions for the superconducting surface impedance have been worked out in detail by Mattis and Bardeen¹²) and Abrikosov, Gorkov, and Khalatnikov¹³). These expressions are in a rather difficult form to obtain numerical values. The latter authors have reduced their expressions in the Pippard limit to an approximate form for $\hbar\omega < \Delta$ and $k_B T \ll \Delta$. Detailed computer pro-

grams have been developed by the author¹⁴⁾ using the expression of Mattis and Bardeen and by Halbritter^{15),16)} using a Green's function formalism¹⁷⁾. The approximate frequency and temperature dependences are as follows:

$$R_{BCS} \propto \omega^{1.7} \exp(-\Delta/k_B T) \quad (5)$$

PENETRATION OF FIELD INTO SUPERCONDUCTOR

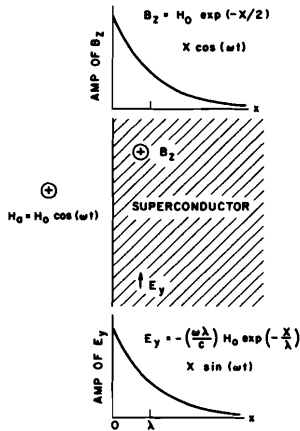


Fig. 3. Approximate representation of the penetration of the magnetic and electric fields into a BCS superconductor.

Detailed comparisons of the experimental surface resistance have been made with the theoretical expressions for the BCS surface resistance for a number of superconductors.^{14),7)18)} Figure 4 shows an example of the comparison of experimental data for Nb at 11 GHz with theoretical calculations as a function of temperature⁷⁾. It is seen that the theoretical calculations fit the experimental data over four orders of magnitude. Figure 5 shows an example of a comparison of the experimental data of Pierce⁵⁾ and Szecs¹⁹⁾ for Pb at 4.17°K with the calculations of Halbritter¹⁸⁾ as a function of frequency. Again the calculations fit the data quite well. The BCS surface resistance can be regarded as generally well understood, and it can be calculated to better than 20% in most cases.

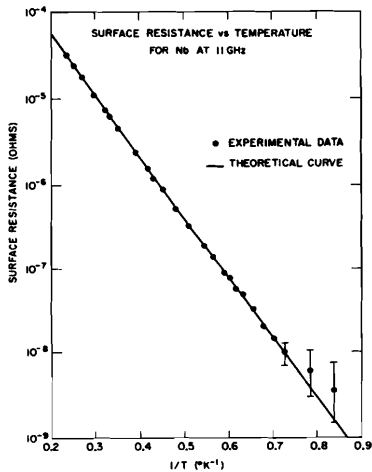


Fig. 4. Comparison of experimental and theoretical surface resistance as a function of temperature for Nb at 11 GHz.

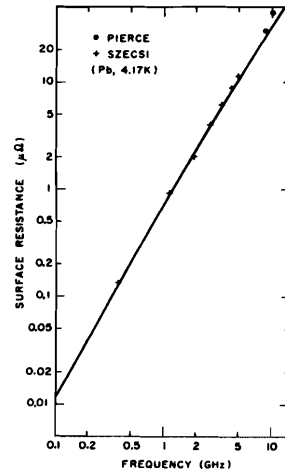


Fig. 5. Comparison of experimental and theoretical surface resistance as a function of frequency for Pb at 4.17°K.

4. The Residual Surface Resistance

In experimental measurements, it is always observed that the surface resistance approaches a finite non-zero value as $T \rightarrow 0^\circ K$. In fact, when one compares experiment with the BCS surface resistance, the relationship

$$R_{exp} = R_{BCS} + R_{resid} \quad (6)$$

is generally assumed. R_{resid} , which for most important contributions is only weakly dependent on temperature, characterizes those dissipation mechanisms that are due to other than the BCS dissipation. Quite often the residual dissipation may be localized on the superconducting surface to a few small regions. One must keep this fact in mind since most experimental R_{resid} quoted in the literature are determined assuming R_{resid} is

uniform over the surface. R_{resid} can be the result of factors over which one in principle has experimental control as well as factors which are an inherent solid state property of the superconductor.

The possible dissipation mechanisms giving rise to a R_{resid} are many; however, the verification of a specific dissipation mechanism is difficult. An example of a relatively well understood source of R_{resid} is that due to trapped magnetic flux in a superconductor. If one applies an ambient dc magnetic field to a cavity while it is cooled through T_c into the superconducting state, magnetic flux will be trapped in the superconductor. For those small regions where the magnetic flux leaves the surface of the superconductor, the superconducting state is degraded. These small regions have a surface resistance on the order of that for the normal state in the anomalous limit. Experiments have been carried out which demonstrate that R_{resid} (in the average sense for the whole cavity surface) is proportional to the ambient magnetic field and hence to the trapped magnetic flux. Figure 6 shows such a set of data for Pb at 11 GHz⁶⁾ (R_{resid} is proportional to $1/Q_H$). For Nb cavities, R_{resid} has been found to be proportional to the ambient magnetic field squared^{20),21)}. This different dependence on ambient magnetic field may be related to a partial Meissner effect of the thick walled massive Nb cavities used in these experiments or perhaps to the tendency in type II superconductors (Nb) for the trapped flux to isolate itself into individual flux quanta at low field.

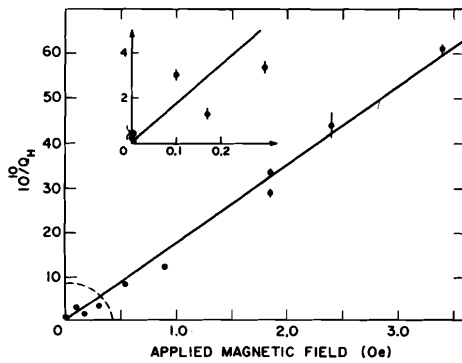


Fig. 6. The residual $Q(Q_H)$ as a function of ambient magnetic field during transition into superconducting state for an electroplated Pb cavity at 12 GHz.

Dielectric losses giving rise to a R_{resid} have been also clearly observed in superconducting cavities. By dielectric loss, one means that loss which is proportional to E^2 on the surface rather than H^2 . This type of loss became clear when it was found that cavities with large electric fields

on their surfaces (e.g. TM_{010} mode) were much more susceptible to increased R_{resid} as the result of poor vacuum than cavities without large electric fields on their surfaces (e.g. TE_{011} mode). For example it was possible to reach a Q_0 of 10^{10} in a TE_{011} mode Nb cavity with only an oil mechanical pump vacuum⁷⁾, but ultra-high-vacuum techniques were required for TM_{010} mode Nb cavities²²⁾.

One rather intriguing example of a residual dissipation mechanism, which Halbritter²³⁾ has shown may be important, is phonon generation. Phonon generation is an inherent solid state property of a superconductor. There are several coupling mechanisms for phonon generation. The two more important are the coupling of the electric field parallel to the surface to the ions in the superconductor and the coupling of the electric field perpendicular to the surface to the electric dipole at the surface of the superconductor. The first type of coupling may be enhanced by surface roughness. The frequency dependence of phonon generation may be from ω^0 to ω^2 .

There are, of course, additional proposed mechanisms for residual dissipation: examples are small normal regions and regions of degraded superconductivity due to imperfections, magnetic impurities, surface roughness, and trapped flux due to thermal electric currents. It is very difficult to verify experimentally these different dissipation mechanisms since they depend on a good knowledge of microscopic properties of the superconductor. Unfortunately, the important contributions to R_{resid} are not very well understood since it is due to those mechanisms over which we have not established experimental control. Nevertheless in a variety of circumstances residual surface resistances of a few times $10^{-9}\Omega$ have been achieved^{9),24),25),26)}.

5. Non-Linear Effects

5.1 The Surface Resistance

Only the surface resistance for low fields has so far been discussed. As the fields in a cavity are increased a non-linear contribution to the surface resistance can occur (i.e., the power dissipation follows a dependence on H other than H^2). The BCS surface resistance itself increases with magnetic field due to the degradation of the superconductivity with magnetic field. R_{BCS} increases (for $T < 0.5 T_c$) principally as the result of the energy gap decreasing with magnetic field. Although for Pb and Nb the decrease in the energy gap is small, the fact that it occurs in the exponential leads to an important increase in R_{BCS} . The increase in R_{BCS} has been calculated using the Ginzburg-Landau theory for superconductivity^{27),28)}. The non-linear R_{BCS} can be expressed as follows:

$$R_{BCS}(H) = R_{BCS}(0) \left[1 + \gamma \left(\frac{H}{H_c} \right)^2 \right] \quad (7)$$

At 2°K, $R_{BCS}(H_c)/R_{BCS}(0)$ for Pb is about 2 and for Nb is about 4.

There are a number of other non-linear dissipation mechanisms that are known. There is additional dissipation for certain magnetic field levels due to surface states²⁹). Surface states result from the modification of the electron states near the surface by the magnetic field and specular reflection. It is felt that experimental information qualitatively verifies the existence of these surface states. Another important example is the non-linear surface resistance due to phonon generation by the pressure produced from the interaction of a normal electric field with its induced surface charge and the interaction of a parallel magnetic field with its induced surface current. The author has estimated that a magnetic field of 1500 Oe could lead to a R_{resid} of about $3 \times 10^{-9} \Omega$ due to non-linear phonon generation. At the highest frequencies and fields multiple photon absorption may become important. Also one may observe an increase in the surface resistance with field resulting from the finite thermal conductivity of the superconductor and the consequent temperature rise. Experimental work is needed to verify the importance of the various non-linear dissipation mechanisms.

5.2 Frequency Tuning Effects

Although small changes in the surface reactance with field do not appear to be an important consideration in superconducting accelerator design, frequency tuning from the static radiation pressure can be very important. The static radiation pressure is proportional to field squared. Frequency shifts which can be accounted for by the cavity deformation due to the radiation pressure have been observed⁸). Disk loaded accelerator structures can generally be made strong enough to limit the frequency shifts to a few bandwidths, but other types of cavities are very sensitive to the radiation pressure. A $\delta f/f$ as high as 0.01 has been reported³⁰).

In addition to static frequency shifts, coupling due to the radiation pressure between rf cavity modes and mechanical modes in helical cavities have been observed³¹). With active feedback these coupled oscillations have been suppressed to very high fields³²).

6. RF Critical Magnetic Field

Figure 7 shows a typical graph of Q_0 as a function of field⁶). It is observed that at a certain field, called the rf critical magnetic field H_c^{rf} , an instability in Q_0 occurs. The term H_c^{rf} refers to the peak rf magnetic field on the surface. In Fig. 7, it is seen that the Q_0 drops from 2×10^{10} to 4×10^5 at about 700 Oe. H_c^{rf} can usually be reached either cw or for pulses of a few 10^{-3} s duration. In some cases, however, heating effects are important in which case one can reach higher fields with short pulses. This situation will not be discussed since it does not appear

to be an inherent property of a superconductor and occurs only occasionally. At H_c^{rf} the Q_0 switches to its lower value typically in about $1 \mu s$. The Q_0 recovers only after the field reaches a low value and the surface temperature recovers. The H_c^{rf} has been explained both on the basis of thermal runaway and partial phase transition of the superconducting state with subsequent thermal runaway. An approximate calculation of thermal runaway has been made assuming a small region of high surface resistance is located on an otherwise superconducting surface³³); however, more detailed calculations need to be made.

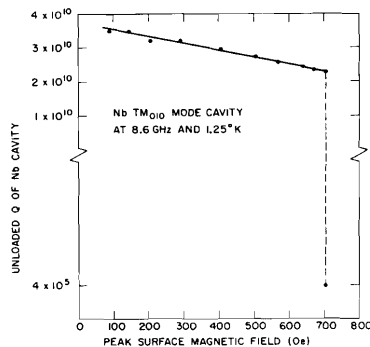


Fig. 7. The unloaded Q of a Nb cavity at 8.6 GHz as a function of peak surface magnetic field.

Here the H_c^{rf} initiated by a partial phase transition will be discussed in detail. The dynamics of the transition are not well understood at microwave frequencies; however, for the frequencies of interest one can learn a great deal by considering the dc magnetic properties of a superconductor. This approach is reasonable because experimental evidence³⁴) indicates that the switching time of a thin superconductor to the normal state occurs in less than 5×10^{-11} s (much faster than one rf period at 10^{10} Hz). In a bulk superconductor, one only needs a large increase in the number of electrons thermally excited across the gap (a partial phase transition) near the surface of the superconductor since this increase will lead to a subsequent thermal runaway. The rf critical magnetic field will be discussed separately for type I and type II superconductors.

6.1 Type I Superconductors

A type I superconductor is one which has a positive surface free energy at the surface between regions of normal and superconducting states. In the Ginzburg-Landau theory, it is a superconductor with a κ value less than $1/\sqrt{2}$. Pb and Sn are examples of type I superconductors. Figure 8 shows the ideal magnetic behavior of a type I superconductor. If the superconductor is initially in the superconducting state at zero field, the superconducting state will persist until the magnetic field reaches the superheating magnetic field H_{sh} , above which the superconductor will go into the normal state. If the magnetic field is then decreased, the normal state will persist until the supercooling magnetic field is reached, below which the superconductor will go into the superconducting state. The hysteresis type behavior is due to the positive surface free energy. The volume free energies of the superconducting and normal states are equal at the thermodynamic critical magnetic field H_c ; however, either the superconducting or normal states can persist in the region between H_{sc} and H_{sh} because the normal and superconducting states can not spontaneously nucleate in this field region. Real superconductors, however, generally contain imperfections which act as nucleation sites. Thus in real superconductors the phase transition usually always occurs close to H_c .

IDEAL MAGNETIC BEHAVIOR OF TYPE I SUPERCONDUCTOR

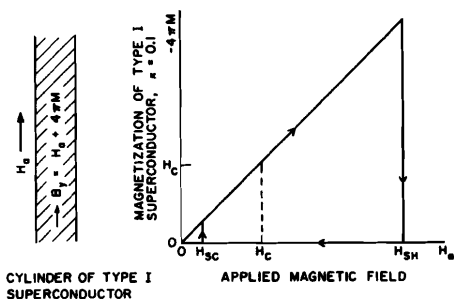


Fig. 8. Ideal magnetic behavior of type I superconductor.

From the dc magnetic behavior of a type I superconductor, one would expect that H_c^{rf} would be near H_c . This statement would be expected to be true even if there were some surface roughness giving rise to field enhancement: (1) a point at which the magnetic field is enhanced may be ideal and may not begin to go normal until H_{sh} is reached, and (2) if such a point did go into the normal state, the normal state would not propagate since the average magnetic field is less than H_c (of course thermal runaway might occur if

the normal region were too large). If the rf magnetic field were greater than H_c , a small normal nucleus would expand and thermal runaway would eventually occur.

The above view is verified by experiment. Figure 9 shows the measured H_c^{rf} for Sn at 2.85 GHz along with the dc H_c (14). It is clear that H_c^{rf} and H_c are in relatively good agreement. Measurements for Pb have given similar results (35). H_c^{rf} have, of course, been measured for type I superconductors below H_c ; however, these H_c^{rf} were probably limited by heating effects rather than any inherent property of the superconductor.

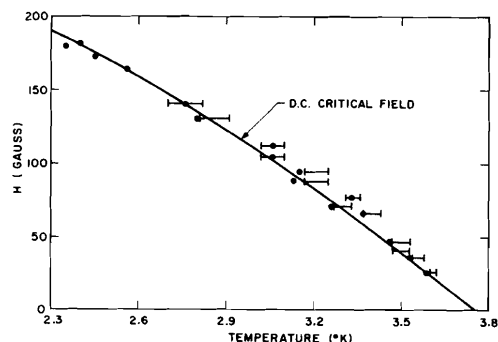


Fig. 9. The rf critical magnetic field of Sn as a function of temperature. The data points are represented by \bullet and \blacksquare , and the dc critical magnetic field is represented by the solid curve.

6.2 Type II Superconductors

A type II superconductor is one which has a negative surface free energy at the surface between regions of normal and superconducting states. For a type II superconductor, κ is greater than $1/\sqrt{2}$. Nb is an example of a type II superconductor. Figure 10 shows the ideal magnetic behavior of a type II superconductor (for Nb). In this case the magnetization curve is completely reversible. The definition of H_c is the same as for a type I superconductor. A type II superconductor exists in the mixed state between H_{c1} and H_{c2} . In the mixed state, there are both normal and superconducting regions in the superconductor. There is an additional detail not shown in Fig. 10. There is a superheating magnetic field associated with H_{c1} , which has a value of about H_c (36). This different type of superheating magnetic field is associated with the increased potential energy of a fluxoid near the surface of a superconductor. For real type II superconductors, the electron mean free path and hence the impurity level in the superconductor has a very important effect on H_{c1} and H_{c2} : with decreased electron

mean free path H_{c1} decreases and H_{c2} increases.

7. Electron Loading Effects

In addition to the surface dissipations that were discussed above, there can be dissipation associated with the production of electrons, the acceleration of these electrons in the rf electric field, and their eventual collision with the walls. The two principal processes by which electron loading occur are electron field emission and electron multipactoring. These electron loading effects will not be considered in much detail since they are not peculiar to superconducting cavities. The interaction of a particle beam with rf cavity will not be discussed.

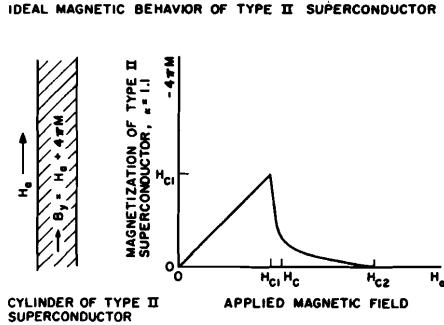


Fig. 10. Ideal magnetic behavior of type II superconductor.

For a type II superconductor, one might believe that H_c^{rf} would occur at H_{c1} since the normal state can nucleate at this field level and hence the surface resistance would increase with subsequent thermal runaway. In actual fact, however, only much lower fields have been reached with superconducting Nb surfaces: 1080 Oe at 8.6 GHz³¹, 554 Oe at 2.3 GHz³⁷, 300 Oe at 1.3 GHz, and 1000 Oe at 90 MHz³². Thus the highest H_c^{rf} for Nb is about 0.6 H_{c1} . The possible explanations for the lower H_c^{rf} for Nb are several: (1) the surface current is much larger at H_{c1} and thus thermal runaway from dissipation is more likely, (2) since there is no H_{sh} , local field enhancement due to roughness can lead to an increased surface resistance when the local field exceeds H_{c1} , and (3) impurities and crystal imperfections can lead to locally depressed values of H_{c1} .

The data quoted above suggests H_c^{rf} depends on area with a larger area resulting in a lower H_c^{rf} . (The 90 MHz helical cavity has an active surface area similar to that of the 8.6 GHz cavity.) This result and the fact that H_c^{rf} varies from cavity to cavity (100 Oe to 1080 Oe for 8.6 GHz Nb cavities) suggests that a statistical model of imperfection may explain the general decrease in H_c^{rf} with area. However, recent measurements at Stanford on a 23-cell 1.3 GHz cavity indicate that for very large area cavities H_c^{rf} no longer decreases rapidly with area since a field of 200 Oe was obtained in this cavity.

7.1 Electron Field Emission

Electron field emission (efe) has been studied in detail at dc. Efe is the tunneling of electrons through a potential barrier at the surface of a conductor. One should, in principal, be able to reach fields well in excess of 100 MV/m before a significant efe current would occur. However, in dc efe measurements it is observed that very large efe currents flow at relatively low electric fields. These large efe currents at low electric fields are explained by electric field enhancement at microscopic projections³⁰. (The large efe currents could also be explained by a reduced work function.) The electric field enhancement is measured by the field enhancement factor β , which is defined as E_{loc}/E_{av} . E_{loc} is the peak local electric field on a projection, and E_{av} is the average electric field on the surface. β can be measured by making Fowler-Nordheim plots of the efe current and E_{av} ³⁸. Typical values of β at dc for unprocessed large area surfaces are a few hundred.

Electron field emission in rf cavities is not significantly different from dc except that one must of course take an appropriate time average of the efe current. In cavities it has not been possible to measure the efe currents directly, but the dependence of the efe current on electric field can be measured indirectly by the x-radiation produced when the electrons collide with the walls. Using the x-radiation as a measure of the efe currents does produce some difficulties in making Fowler-Nordheim plots; however, the corrections do not appear to be too large. For a Nb cavity at 1.3 GHz, β of from 200 to 400 are typically measured³⁹. Also it has been possible to decrease β by He-ion sputter processing: in one case from 450 to 170³⁹.

7.2 Electron Multipactoring

Electron multipactoring has been adequately discussed before⁴⁰. For a superconducting cavity it is not allowed since it increases the heat dissipation at low temperatures. A few interesting facts have been observed for electron multipactoring in superconducting cavities: it is possible to process the cavity surface by allowing electron multipactoring to occur with the result that the phenomena disappears^{40,39}, the electrons involved in

multipactoring appear in some cases to have energies on the order of 100 keV when they collide with the wall³⁹⁾ (in multipactoring, electrons usually have an energy on the order of 1 keV), and anodizing enhances multipactoring^{40),39)}. In some cases reactive loading of electron multipactoring can lead to important frequency shifts for superconducting accelerating devices. For many types of cavities, electron multipactoring can be avoided by slight alterations in cavity geometry.

8. Conclusion

Our present understanding of rf superconductivity indicates that it should be possible in principle to reach electric fields in excess of 100 MV/m and peak surface magnetic fields of about H_c for Pb (750 Oe at 1.8°K) and H_{c1} for Nb (1750 Oe at 1.8°K). For Nb at 8.6 GHz, values not far from these have been achieved: 70 MV/m and 1080 Oe. However for large cavities dirt effects that are not intrinsic to the superconductor are experienced. Progress will be made for large cavities by improvement of surface treatments, crystal structure and purity, and fabrication techniques.

Not much work has yet been done on radiation damage of rf superconducting cavities and other sorts of long term degradation effects. The recent work on radiation damage by Halama³⁷⁾ is encouraging since it indicates radiation can be tolerated in some instances.

References

* Work supported in part by the U.S. Office of Naval Research, Contract N00014-67-A-0112-0061 and the National Science Foundation.

- (1) E. Jones, private communication.
- (2) L. R. Suelzle, *IEEE Trans. Nucl. Sci.* NS-18, No. 3, 146 (1971).
- (3) A. Citron, Proc. 1970 Proton Lin. Acc. Conf. NAL, Batavia, Vol. I, 239 (1970).
- (4) A. O. Hanson, *IEEE Trans. Nucl. Sci.* NS-18, No. 3, 149 (1971).
- (5) H. A. Schwettman, P. B. Wilson, J. M. Pierce, and W. M. Fairbank, *International Advances in Cryogenic Engineering*, Vol. 10 (Plenum Press, New York, 1965) p. 88.
- (6) J. M. Pierce, HEPL Report No. 514 (W. W. Hansen Laboratories of Physics, Stanford University, Stanford, Calif. 1967).
- (7) J. P. Turneaure and Ira Weissman, *J. Appl. Phys.* 39, 4417 (1968).
- (8) J. P. Turneaure and Nguyen Tuong Viet, *Appl. Phys. Lett.* 16, 333 (1970).
- (9) H. Martens, H. Diepers, R. K. Sun, *Phys. Lett.* 34A, 439 (1971).
- (10) P. Kneisel, O. Stolz, J. Halbritter, H. Diepers, H. Martens, R. K. Sun, this conference.
- (11) J. Bardeen, L. N. Cooper, and J. R. Schrieffer, *Phys. Rev.* 108, 1175 (1957).
- (12) D. C. Mattis and J. Bardeen, *Phys. Rev.* 111, 412 (1958).
- (13) A. A. Abrikosov, L. P. Gorkov, and I. M. Khalatnikov, *Soviet Phys. - JETP* 8, 182, (1959).
- (14) J. P. Turneaure, HEPL Report No. 507 (W. W. Hansen Laboratories of Physics, Stanford University, Stanford, Calif., 1967).
- (15) J. Halbritter, *Externer Bericht* 3/69-2 (Kernforschungszentrum, Karlsruhe, 1969).
- (16) J. Halbritter, *Externer Bericht* 3/70-6 (Kernforschungszentrum, Karlsruhe, 1970).
- (17) A. A. Abrikosov, L. P. Gorkov, and I. Ye. Dzyaloshinski, *Quantum Field Theoretical Methods in Statistical Physics* (Pergamon Press, Oxford, 1965).
- (18) J. Halbritter, *Z. Physik* 238, 466 (1970).
- (19) L. Szeesi, *Externer Bericht* 3/70-8 (Kernforschungszentrum, Karlsruhe, 1970).
- (20) C. Lyneis, private communication.
- (21) P. B. Wilson, M.A. Allen, H. Deruyter, V. D. Farkas, H. A. Hogg, E. W. Hoyt, and M. Rabinowitz, this conference.
- (22) Ira Weissman and J. P. Turneaure, *Appl. Phys. Lett.* 13, 390 (1968).
- (23) J. Halbritter, *J. Appl. Phys.* 42, 82 (1971).
- (24) H. J. Halama, *IEEE Trans. Nucl. Sci.* NS-18, No. 3, 188 (1971).
- (25) J. P. Turneaure, *IEEE Trans. Nucl. Sci.*, NS-18, No. 3, 166 (1971).
- (26) Nguyen Tuong Viet, private communication.
- (27) H. A. Schwettman, J. P. Turneaure, W. M. Fairbank, T. I. Smith, M. S. McAshan, P. B. Wilson, and E. E. Chambers, *IEEE Trans. Nucl. Sci.* NS-14, No. 3, 336 (1967).
- (28) J. Halbritter, *Externer Bericht* 3/68-8 (Kernforschungszentrum, Karlsruhe, 1968).
- (29) J. Halbritter, *Externer Bericht* 3/70-14 (Kernforschungszentrum, Karlsruhe, 1970).
- (30) M. Kuntze, private communication.
- (31) D. Schulze, H. Strube, K. Mittag, B. Piosczyk, and J. Vetter, *IEEE Trans. Nucl. Sci.* NS-18, No. 3, 160 (1971).
- (32) A. Citron, J. L. Fricke, H. Klein, M. Kuntze, B. Piosczyk, D. Schulze, H. Strube, J. E. Vetter, and C. M. Jones, this conference.
- (33) D. Leroy, private communication.
- (34) J.I. Gittleman and S. Bozowski, *Phys. Rev.* 135, A297 (1964).
- (35) Y. Bruynseraede, D. Gorle, D. Leroy, and P. Morignot, to be published.
- (36) Pierre G. deGennes, *Superconductivity of Metals and Alloys* (Benjamin, New York, 1966).
- (37) H. J. Halama, this conference.
- (38) D. Alpert, D. A. Lee, E. M. Lyman, and H. E. Tomaschke, *J. Vac. Sci. Tech.* 1, 35 (1964).
- (39) J. P. Turneaure, J. F. Crawford and I. Ben-Zvi, to be published.
- (40) G. Dammertz, H. Hahn, J. Halbritter, P. Kneisel, O. Stoltz, J. Votruba, and H. Diepers, *IEEE Trans. Nucl. Sci.* NS-18, No. 3, 181 (1971).

DISCUSSION

H. LENGELER : Could you make a comment on other surface treatments like anodizing.

coating to lower the emission rate of electrons from the surface ?

J. TURNEAURE : Anodization of Nb appears to be a very promising surface treatment for at least some applications. Anodized Nb cavities have reached Q's and fields of the same order as for Nb cavities fired in an UHV furnace. The principal advantage of anodized Nb is that one need not have available an expensive UHV furnace. However, anodized Nb surfaces have been shown to have much more difficulty with electron multipactoring than UHV fired surfaces. Further, some people have made the suggestion that anodized Nb surface will be more subject to various types of degradation of its r.f. properties in time. Halama at Brookhaven has experimental information that indicates anodized Nb surfaces are more subject to radiation damage than UHV fired Nb surfaces.

J. TURNEAURE :

1. In some circumstances electron field emission may still be a problem rather than a critical magnetic field. This question will depend on the ratio of peak electric to magnetic field for a particular cavity as well as other factors. I was referring to the 1.3 GHz Nb accelerator structure at Stanford. In this case we are able to increase the field at which excessive electron field emission occurs by He-ion sputter processing. A paper will be available on this work shortly. Also further improvements in electrochemical polishing are expected to reduce electron field emission, but this has not yet been demonstrated.

E.G. KOMAR : What is the experimental value of Q now ?

2. At Stanford we have not thought of applying a protective coating to the Nb surface. However, at other laboratories this possibility has been considered. The experience with anodized Nb, which may be considered to have a protective layer, is that electron field emission is not much different from that of UHV fired Nb.

J. TURNEAURE : Unloaded Q's of just over 10^{11} have been achieved in X-band TM_{010} mode Nb cavities and a re-entrant S-band Nb cavity. In most other situations ($10^8 - 10^{10}$ Hz), Q's of generally a few times 10^{10} have been achieved.

T.K. KHOE : Why is the residual resistance R_{Res} much more difficult to reduce at lower frequency (~ 100 MHz) than at high frequency 2 GHz ?

C. GERMAIN : The improvement of voltage holding capability you mentioned, on injecting gas to a pressure of a few 10^{-4} torr, due to reduction of the field enhancement factor of the microgeometry by ion sputtering of the points, has been used for years in electrostatic separators. But this improvement lasts only as long as there is a higher pressure in the tank. Do you contemplate using a higher pressure or semi-vacuum, permanently in your cavity and, if not, how long does this effect last ?

J. TURNEAURE : The answer to this depends on how one states the question. In fact, experimentally achieved residual surface resistances at 100 MHz are as low as have been achieved in the range 1 - 10 GHz. It is another question to ask why one does not get the same large improvement factor between 4.2°K and 1.8°K for 100 MHz that is obtained at 10 GHz. This is, of course, related to the frequency dependence of the type of loss mechanism that gives rise to the residual surface resistance and not to the frequency dependence of the BCS surface resistance ($\omega^{1.7}$). The frequency dependence of the residual surface resistance can vary from ω^0 to ω^2 depending on the proposed loss mechanism : phonon generation can lead to a frequency dependence anywhere from ω^0 to ω^2 , normal regions and trapped flux lead to a frequency dependence of about $\omega^{2/3}$, etc. It may also be that the greater fabrication and processing difficulties of the lower frequency cavities contribute to the residual surface resistance.

J. TURNEAURE : We do not intend leaving the He gas in the cavity after He-ion sputter processing. Our experience is different from that related to electrostatic separators. In microwave cavities at 1.3 GHz, the reduced field enhancement factor appeared to be indefinite without the presence of He gas. The tests in these cavities have lasted for several weeks.

J. VETTER : Two questions :

H. LENGELER : We heard from Dr. K. Green that progress in pulsed S.C. magnets has had ups and downs but now real progress seems to be being made. What about S.C. Accelerators and Separators.

1. What methods had you in mind when you commented that field emission is not a real problem in achieving high field levels ?

J. TURNEAURE : The work on superconducting r.f. cavities has experienced some "ups and downs". The most prominent of these was the rather rapid progress in obtaining high fields and Q's in X-band Nb cavities and the subsequent difficulty of obtaining similar results in full size Nb accelerator structures. Since beginning the work on full size accelerator structures, the progress has become more even. Progress in other aspects of the superconducting

2. Did you think of applying any protective

accelerator development have been more even throughout.

J.B. ADAMS : Do you think that superconductive cavities offer a practical way of making a linear accelerator ?

J. TURNEAURE : Yes ! However, such a judgement depends on the type of beam that is desired. For instance, the use of superconducting cavities to produce electron beams with only the highest possible energy as the principal criterion is some distance in the future. For the electron linear accelerator being constructed at Stanford, superconducting cavities are practical. In this linac, large duty factor (0.1 - 1), high beam current (100 μ A - 1 mA), and good energy resolution (10^{-4} full width at half max.) are considered important criteria as well as energy (0.2 - 2 GeV). In addition, the characteristics of the linac make it suitable for the recirculation of the beam to obtain energies up to 4 - 6 GeV and this recirculation is being planned.

W.K.H. PANOFSKY : We carried out a study to convert SLAC to a superconducting device but have concluded that gradients near 10 MeV/ft in a travelling wave structure are essential. This, together with the quality-control problem, persuaded us that such a conversion is not attractive. I believe that, as a component in a system where lower gradients are acceptable, the potential is good; also the separator application is attractive.

J.B. ADAMS : Could we ask Dr. Schwettman to make a few comments on recent progress on the superconducting linac ?

H.A. SCHWETTMAN : During the past few months at Stanford we have assembled and tested the injector of our superconducting accelerator. The injector includes a 95 keV room-temperature injector in which the electron beam is chopped and bunched; a superconducting capture section about one meter in length; a superconducting pre-accelerator section about three meters in length; and a beam analysis system. Experiments with this injector system have provided an excellent opportunity to study beam-dynamics problems of the superconducting accelerator and to make engineering tests of all accelerator components under actual operating conditions. These experiments were performed using our superfluid helium refrigerator which is located about 100 meters from the injector system. Thus, the experiments also involved a rather complete test of the entire cryogenic system.

The results of our experiments were extremely encouraging. A 50 μ A electron beam (30 % duty cycle) was accelerated to 6.6 MeV, and the energy resolution was measured to be approximately 0.1 %. The stability of the accelerating fields was demonstrated to be better than one part in 10^4 in amplitude and 0.1° in phase. Our experiments also suggest that loading of the transverse deflection modes to $Q \approx 10^8$ will be adequate to prevent regenerative beam break-up at the 100 μ A level, and that cumulative beam break-up should not be a problem in our 160 meter long superconducting accelerator.